

RELAP5-3D

INTRODUCTION

This paper presents and illustrates some of the key features of the RELAP5-3D code being developed at the Idaho National Engineering and Environmental Laboratory (INEEL) for the US Department of Energy (DOE). The purpose of the paper is to inform potential users of the code of its unique capabilities that extend its range of applicability beyond that presently available with any other thermal-hydraulics systems code. The paper also discusses areas of ongoing development, future plans, and the availability of the code to the international community.

BACKGROUND

The RELAP5-3D code is an outgrowth of the RELAP5/MOD3 code developed at the Idaho National Engineering & Environmental Laboratory (INEEL) for the U.S. Nuclear Regulatory Commission (NRC). Development of the RELAP5 code series began at the INEEL under NRC sponsorship in 1975 and continued through several released versions, ending in October 1997 with the soon to be released RELAP5/MOD3.3. The U.S. Department of Energy (DOE) began sponsoring additional RELAP5 development in the early 1980s to meet its own reactor safety assessment needs. Following the accident at Chernobyl, DOE undertook a re-assessment of the safety of all of its test and production reactors throughout the United States. The RELAP5 code was chosen as the thermal-hydraulic analysis tool because of its widespread acceptance. Systematic safety analyses were carried out for the DOE that included the N reactor at Hanford, the K and L reactors at Savannah River, the Advanced Test Reactor (ATR) at INEEL, the High Flux Isotope Reactor (HFIR) and Advanced Neutron Source (ANS) at Oak Ridge, and the High Flux Beam Reactor (HFBR) at Brookhaven. DOE also chose RELAP5 for the independent safety analysis of the New Production Reactor (NPR) proposed for Savannah River before that program was canceled in the wake of the end of the cold war.

The application of RELAP5 to these various reactor designs created the need for new modeling capabilities. For example, the analysis of the Savannah River reactors necessitated a three-dimensional flow model and heavy water properties be added to the code. ATR required a new critical heat flux correlation applicable to its unique fuel design. All together, DOE sponsored improvements and enhancements have amounted to a multimillion-dollar investment in the code.

Toward the end of 1995, it became clear that the efficiencies realized by the maintenance of a single source code for use by both NRC and DOE were being overcome by the extra effort required to accommodate sometimes conflicting requirements. The code was therefore “split” into two versions, one for NRC and the other for DOE. The DOE version maintained all of the capabilities and validation history of the predecessor code, plus the added capabilities that had been sponsored by the DOE before and after the split.

RELATIONSHIP OF RELAP5-3D TO PRIOR VERSIONS

At the outset of the decision to split the code into NRC and DOE versions, the INEEL recognized the importance of retaining the pedigree stemming from the extensive validation history of RELAP5/MOD3. Consequently, the developmental activities with respect to RELAP5-3D since the split have been carefully integrated so as not to compromise this legacy validation. In fact, virtually all of the enhancements in RELAP5-3D are *optional* and *supplemental* to the proven performance of RELAP5/MOD3.2. Consequently, users of RELAP5-3D can confidently apply the code using existing, one – dimensional RELAP5/MOD3.2 input decks and expect their results to be the same or improved.

To ensure that the code remains true to its validation history (or provides improved results), developmental versions of the code are periodically tested using a subset of cases from the RELAP5/MOD3 validation library. Two such cases are the G.E Level Swell and THTF experiments.

The G.E. Level Swell experiments¹, conducted in the late 1970's provided excellent data for assessing flashing and interphase drag models. Two tanks, one 1 ft. in diameter and the other 4 ft. in diameter were used. In the experiments, the tanks were partially filled with water and heated to near the saturation temperature. They were then depressurized through a blowdown valve. Differential pressure measurements made along the vertical length of the tank allowed for computing average void fractions as a function of elevation inside the tank.

Figure 1 shows the calculated and measured void profiles in the 4 ft. diameter tank of Test 5801-13 at four times during the blowdown (5, 10, 15, and 20 sec.). RELAP5/MOD3.2 and RELAP5-3D produced identical results, both being in excellent agreement with the data.

The Thermal Hydraulic Test Facility (THTF) at Oak Ridge National Laboratory (ORNL) was designed to simulate conditions in a PWR core. The test section contained 64 electrically heated rods with internal dimensions typical of a 17 by 17 rod bundle. Differential pressure measurements positioned along the axial length of the bundle were used to compute void fractions, and thermocouples were employed to measure steam temperature and heater rod surface temperature.

In Test 3.09.10i², the bundle was maintained in a partially uncovered condition at a pressure of 4.5 MPa, an inlet mass flux of 29.8 kg/m²-s, and an inlet subcooling of 57.6 K. The heater rod heat flux (uniform axial and radial) was 7.44x10⁴ W/m². Figure 2 compares RELAP5/MOD3.2 and RELAP5-3D results with measured data for bundle void profile, heater rod temperature profile, and vapor temperature profile. Again, the two code versions are virtually identical and agree well with the data.

The consistency of results between RELAP5/MOD3.2 and RELAP5-3D is not surprising, in light of the fact that the constitutive models for one-dimensional flow have not been significantly altered.

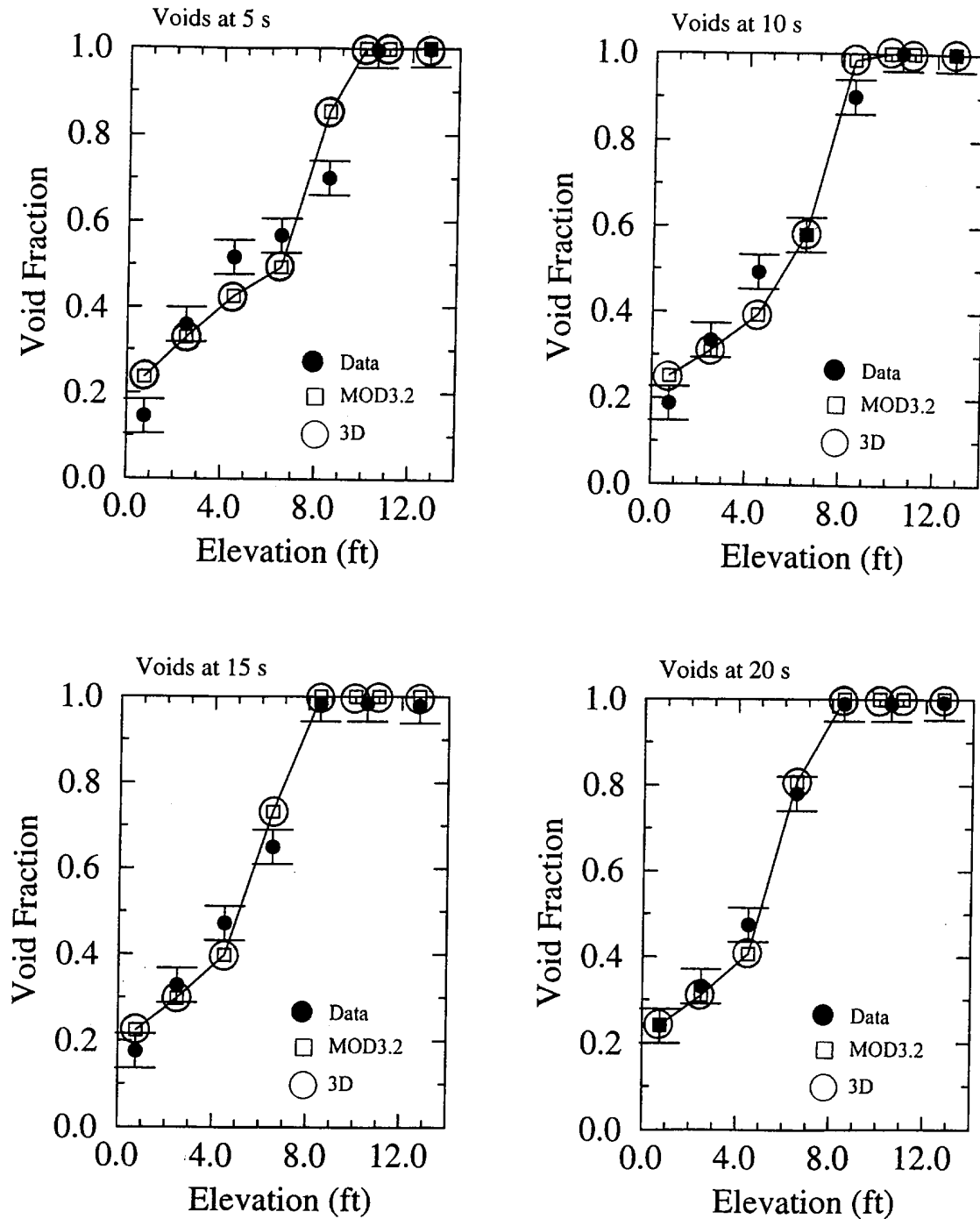


Figure 1. Calculated and Measured Void Profiles During GE Level Swell Test 5801-13

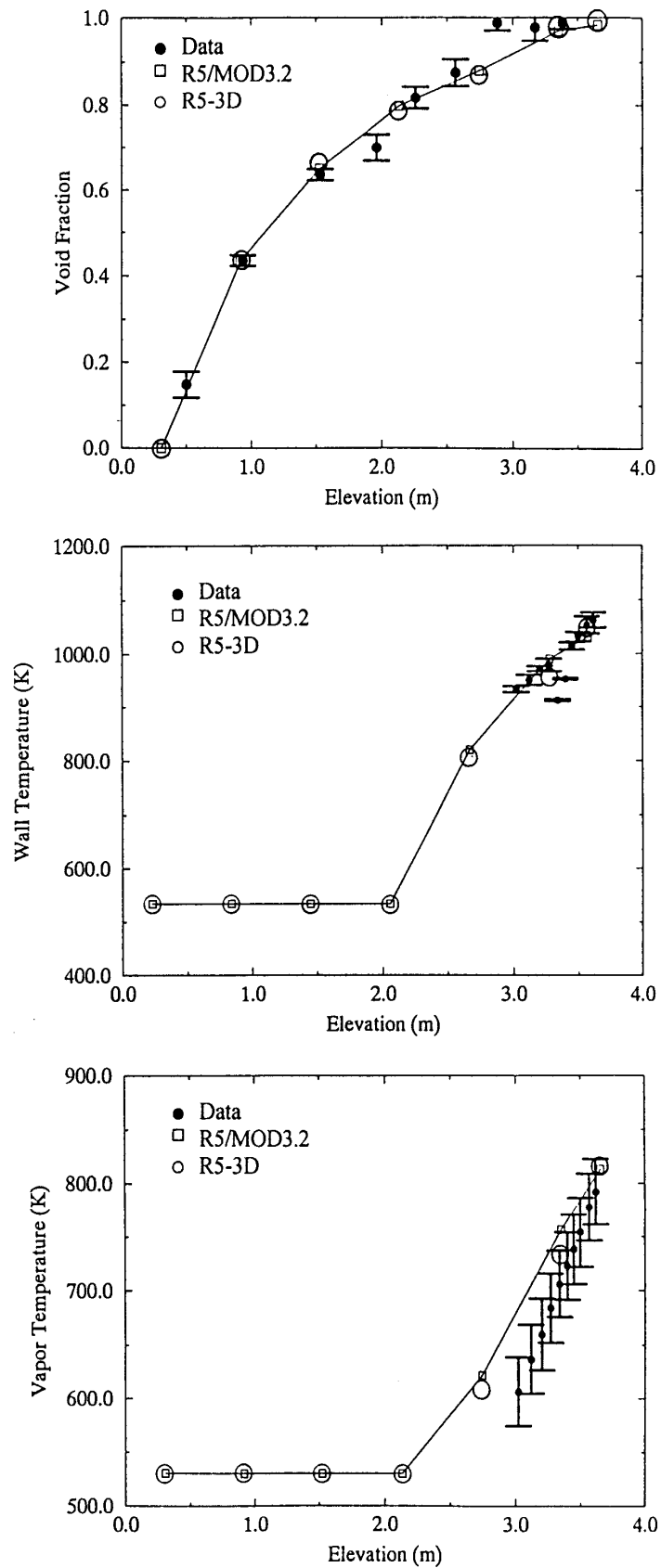


Figure 2. Measured and Calculated Results from THTF Test 3.09.10i

RELAP5-3D CODE FEATURES

The most prominent attribute that distinguishes the DOE code from the NRC code is the fully integrated, multi-dimensional thermal-hydraulic and kinetic modeling capability in the DOE code. This removes any restrictions on the applicability of the code to the full range of postulated reactor accidents. Other enhancements include a new matrix solver, new water properties, and improved time advancement for greater robustness. Together with the existing modeling capabilities of RELAP5/MOD3.2, these enhancements make the code the most powerful tool of its kind available.

The balance of this paper focuses on the capabilities of the three-dimensional hydrodynamic model, the multi-dimensional kinetics model, and the new BPLU matrix solver. Other features unique to RELAP5-3D are briefly described.

Three-Dimensional Hydrodynamic Model

The development of the three-dimensional hydrodynamic model in RELAP5 began in 1990 under funding from the Savannah River National Laboratory (SRNL). Since then development and testing has continued from both planned improvements and responses to user requests. This has resulted in a reliable model. Progress has been documented in the literature and at various meetings (References 3-12).

The multi-dimensional component in RELAP5-3D was developed to allow the user to more accurately model the multi-dimensional flow behavior that can be exhibited in any component or region of a LWR system. Typically, this will be the lower plenum, core, upper plenum and downcomer regions of an LWR. However, the model is general, and is not restricted to use in the reactor vessel. The component defines a one, two, or three-dimensional array of volumes and the internal junctions connecting them. The geometry can be either Cartesian (x, y, z) or cylindrical (r, θ, z). An orthogonal, three-dimensional grid is defined by mesh interval input data in each of the three coordinate directions.

Model Verification

Verification of the model has been performed by using conceptual problems that have exact solutions. These types of problems are used to demonstrate that the equations have been correctly coded, and are a precursor to model validation using experimental data. Three such problems are the “Rigid Body Rotation”, “Pure Radial Symmetric Flow”, and “R- θ Symmetric Flow” problems. Each of the problems is based on a cylindrical, multidimensional component with eight rings, six sectors, and one axial level. All six sectors are symmetrical, with non-uniform radial spacing. Six time dependent volumes are attached to the six outer sectors by time dependent junctions for inlet flow specification. In addition, six time dependent volumes are attached to the six inner sectors by a multiple junction component. Figure 3 shows the nodalization for 1 sector.

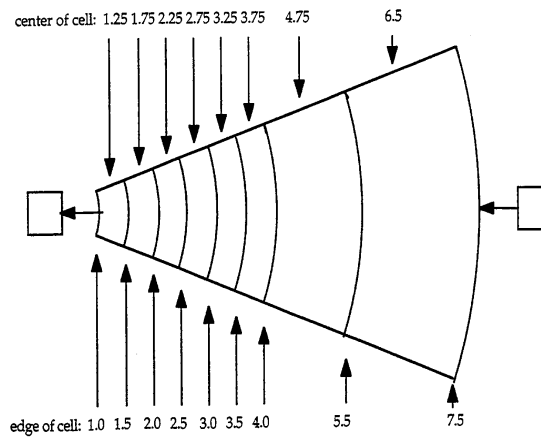


Figure 3. Nodalization of One Sector of Test Problem

In each of the simulations, losses due to friction and body force terms are deactivated to create problems with exact solutions. Also, the flow is assumed to be steady and incompressible. The azimuthal flow pattern, where necessary, was imposed by setting the outer ring azimuthal velocities to the desired value. All problems have analytic solutions for velocity from the continuity and θ -momentum equations, and analytic solutions for pressure from the r-momentum equations.

The Rigid Body Rotation problem represents a hollow cylinder with a symmetric flow pattern in the azimuthal direction. Flow in the radial direction does not exist. This problem tests only the azimuthal momentum flux terms. The test conditions and boundary conditions are: The azimuthal velocity at the 6.5 m radius position is 1 m/s, pressure at the 1 m radius position is 5×10^5 Pa, and all radial velocities are 0.0 m/s.

Comparisons between the RELAP5-3D[®] calculated results and the analytic solution for the Rigid Body Rotation problem are shown in Figures 4 and 5. The calculated velocity and pressure profiles are seen to exactly match the analytical solutions.

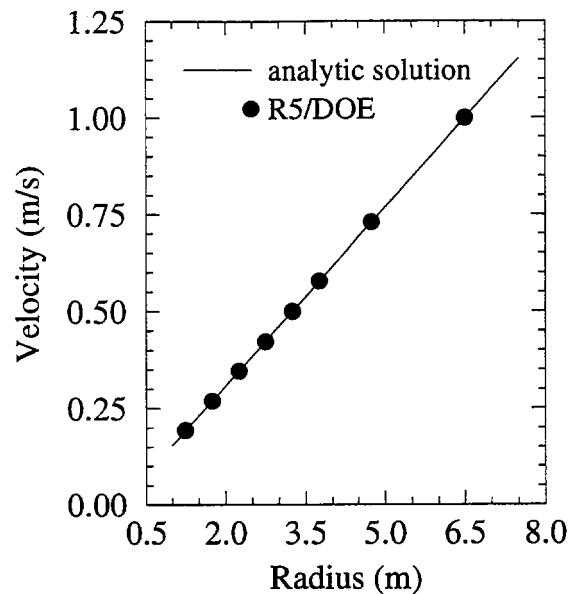


Figure 4. Azimuthal Velocity Profile for Rigid Body Rotation Problem

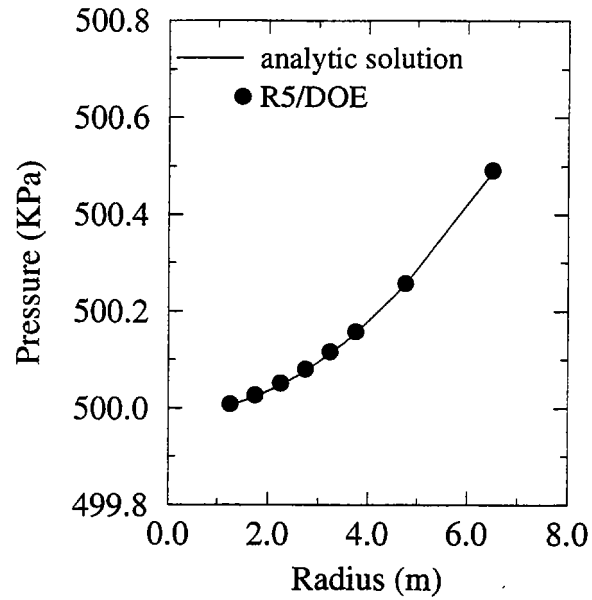


Figure 5. Radial Pressure Profile for Rigid Body Rotation Problem

The Pure Radial Symmetric Flow problem represents a hollow cylinder with a symmetric flow pattern in the radial direction. This problem tests only the radial momentum terms. The test conditions and boundary conditions are: All azimuthal velocities are 0 m/s, pressure at the 1 m radius position is 5×10^5 Pa, and radial velocity at the 7.5 m radius position is 0.8667 m/s (from outside to inside of the ring). Comparisons between the calculated results and the analytic solution for the Pure Radial Symmetric Flow problem are shown in Figures 6 and 7. Again, the RELAP5-3D[®] results are in agreement with the exact solution.

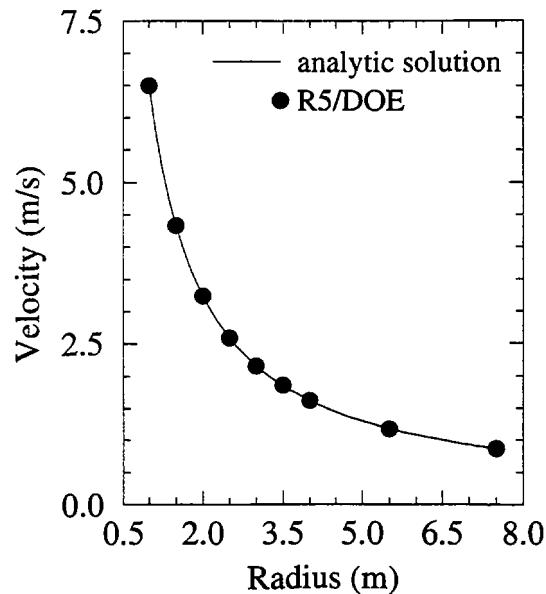


Figure 6. Radial Velocity Profile for Pure Radial Symmetric Flow Problem

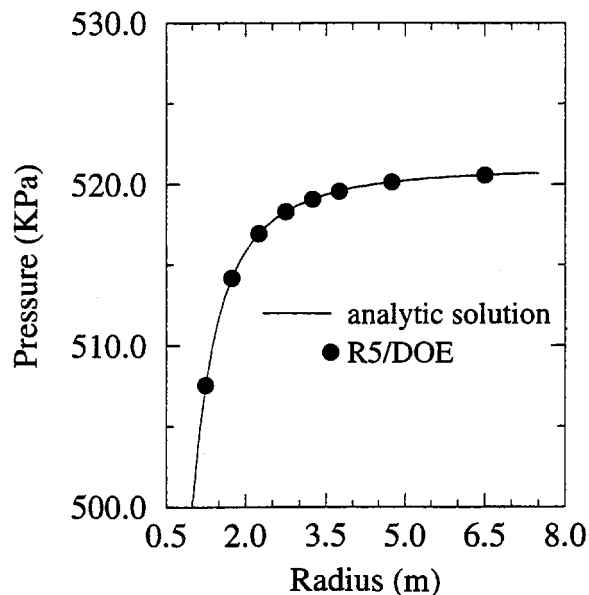


Figure 7. Radial Pressure Profile for Pure Radial Symmetric Flow Problem
 The R- θ Symmetric Flow problem represents a hollow cylinder with a symmetric flow pattern in both the radial and azimuthal directions. The azimuthal velocity at the 6.5 m radius position is 1 m/s, pressure at the 1 m radius position is 5×10^5 Pa, and radial velocity at the 7.5 m radius position is 0.8667 m/s (from outside to inside of the ring). The calculated and analytic solution results are seen to be in agreement (Figures 8, 9, and 10).

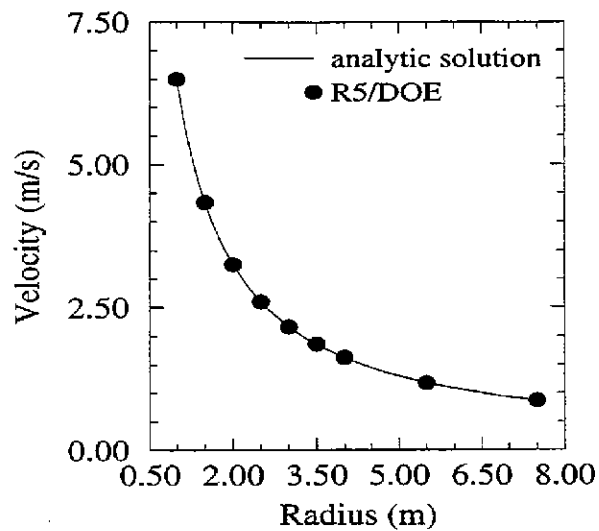


Figure 8. Radial Velocity Profile for R- θ Symmetric Flow Problem

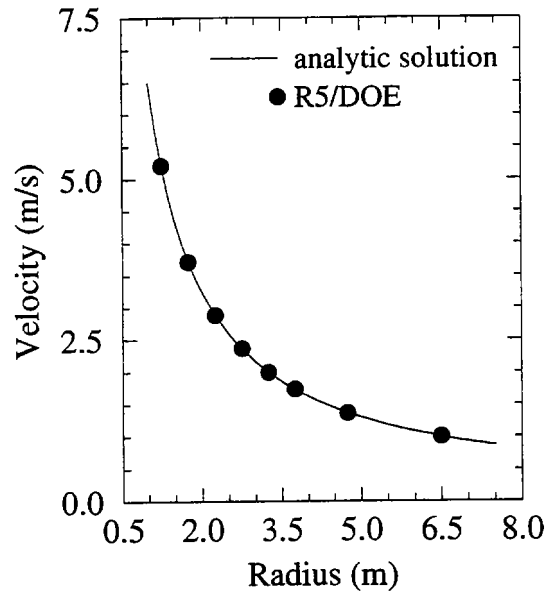


Figure 9. Azimuthal Velocity Profile for R- θ Symmetric Flow Problem

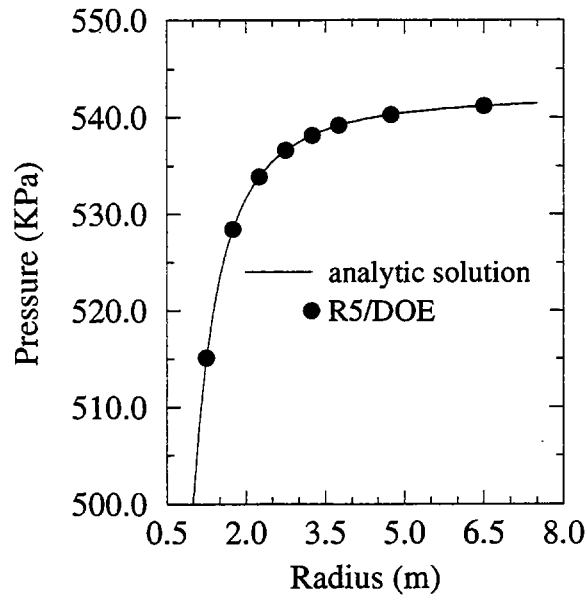


Figure 10. Radial Pressure Profile for R- θ Symmetric Flow Problem

Both the analytic and calculated velocity profiles come from the continuity and θ -momentum equations; they are each a function of radius and outer ring velocity. The velocity profile from the Rigid Body Rotation problem is linear (Figure 4), while the velocity profiles from the other problems are inversely proportional to radius (Figures 6, 8 and 9). The pressures are calculated from the r-momentum equations (Figures 5, 7, and 10). The pressure profile for the Rigid Body Rotation problem is concave up (Figure 5), while the others are concave down. Additionally, the pressure profile from the R- θ Symmetric Flow problem is influenced by the 1-D outlet connections. There, the azimuthal flow contributes to the pressure solution up to the point of connection.

These simple test problems verify the correct implementation of the three dimensional continuity and momentum equations. This is a necessary, but certainly not sufficient, test of the 3D model. Work has begun on performing a number of validation cases using experiments exhibiting multidimensional flow behavior.

Model Validation

One such case recently completed is a simulation of LOFT large break loss-of-coolant-experiment (LOCE) L2-5¹³. The LOFT facility was a 50 MW pressurized water reactor (PWR) that was designed to simulate the response of a commercial PWR during a loss-of-coolant accident (LOCA). Test L2-5 simulated a double-ended offset shear of a cold leg. The experiment was selected because it was judged to provide the most challenging test of the multi-dimensional model of all the experiments in the existing developmental assessment test matrix used for RELAP5/MOD3.

The analysis was accomplished in several steps. First, the original one-dimensional model was upgraded to be consistent with current user guidelines and to better represent Test L2-5. The upgraded one-dimensional model was then run with the current version of RELAP5-3D[®] to obtain baseline results.

The RELAP5/MOD3 model that was used in the developmental assessment of LOFT Test L2-5 is illustrated in Figure 11. The model, hereafter referred to as the one-dimensional model, contains 131 volumes, 142 junctions, and 77 heat structures.

The three-dimensional model of the LOFT reactor vessel was developed using two multi-dimensional components. Multidimensional component 700 represented the downcomer region as shown in Figure 12. Multidimensional component 200 represented the lower plenum, core inlet, core, and upper plenum regions as shown in Figure 13. The vessel was divided into four 90° azimuthal sectors and four radial rings. The four azimuthal sectors corresponded to the four nozzles connecting the loops and the vessel. One radial ring (multidimensional component 700) represented the downcomer while the other three rings (multidimensional component 200) corresponded to high-, average-, and low-powered regions of the core. The axial nodalization of each multi-dimensional component was based on that of the one-dimensional model, resulting in 6 levels for the downcomer and 21 levels for the lower plenum, core inlet, core, and upper plenum regions. A multiple junction (Component 709) connected the bottom of the downcomer to the top of the third ring in the lower plenum. The three-dimensional model of the reactor vessel was then inserted into the one-dimensional model, with the resulting model hereafter referred to as the three-dimensional model.

The core fuel rods were modeled with twelve heat structure geometries, each representing the fuel rods located in a given ring and sector. Each fuel rod heat structure geometry contained twelve heat structures, corresponding to the number of axial levels in the hydraulic nodalization of the core. Each fuel rod heat structure geometry was identical except for its hydraulic connections and the radial power peaking factor. The radial power peaking factors were 1.31, 1.13, and 0.81 for the inner, middle, and outer rings respectively. For comparison, the radial power peaking factors for the high-powered and low-powered rods in the one-dimensional model were 1.31 and 0.94, respectively. The maximum axial power peaking factor was 1.58 and was located in the bottom third of the core.

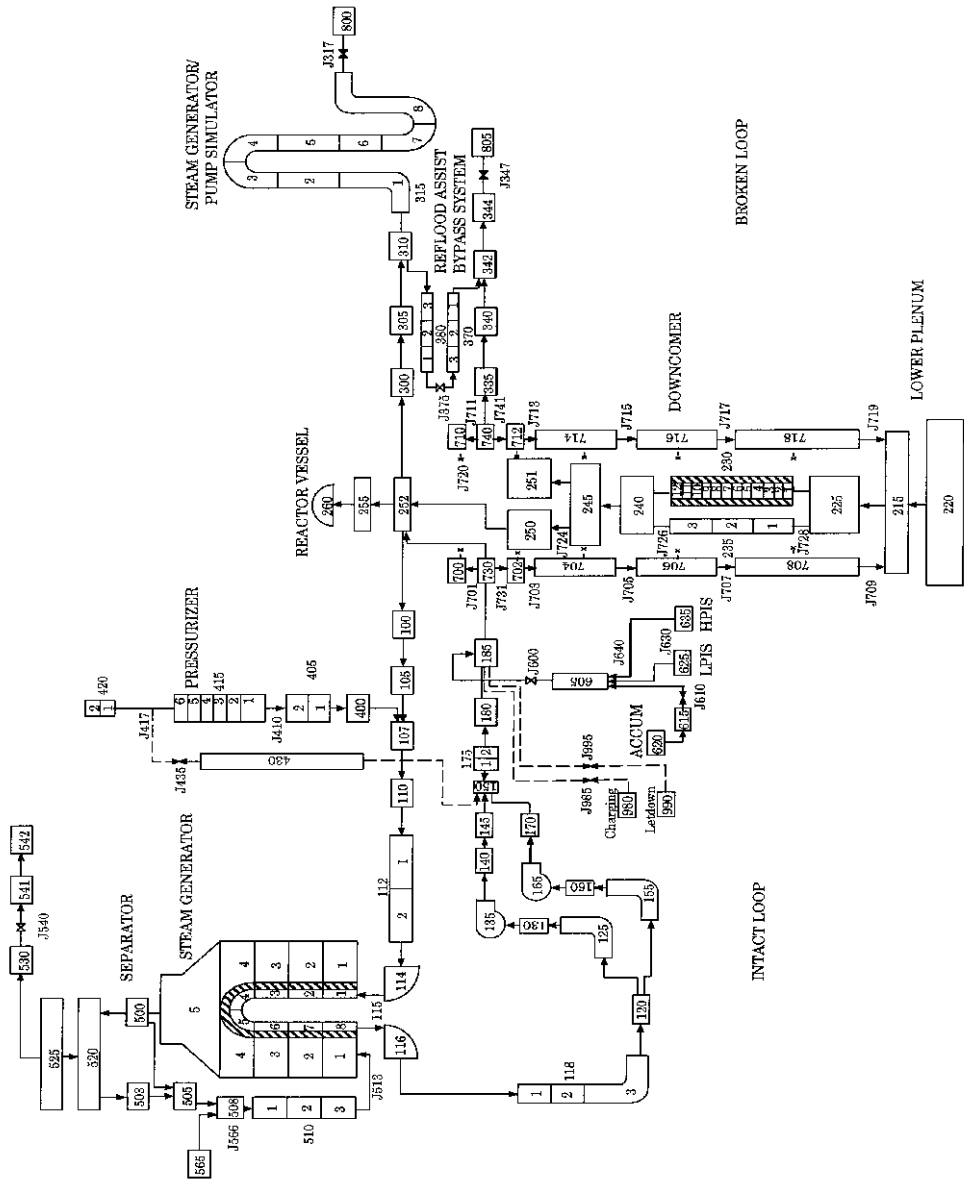


Figure 11. RELAP5/MOD3 Nodalization for LOFT Test L2-5

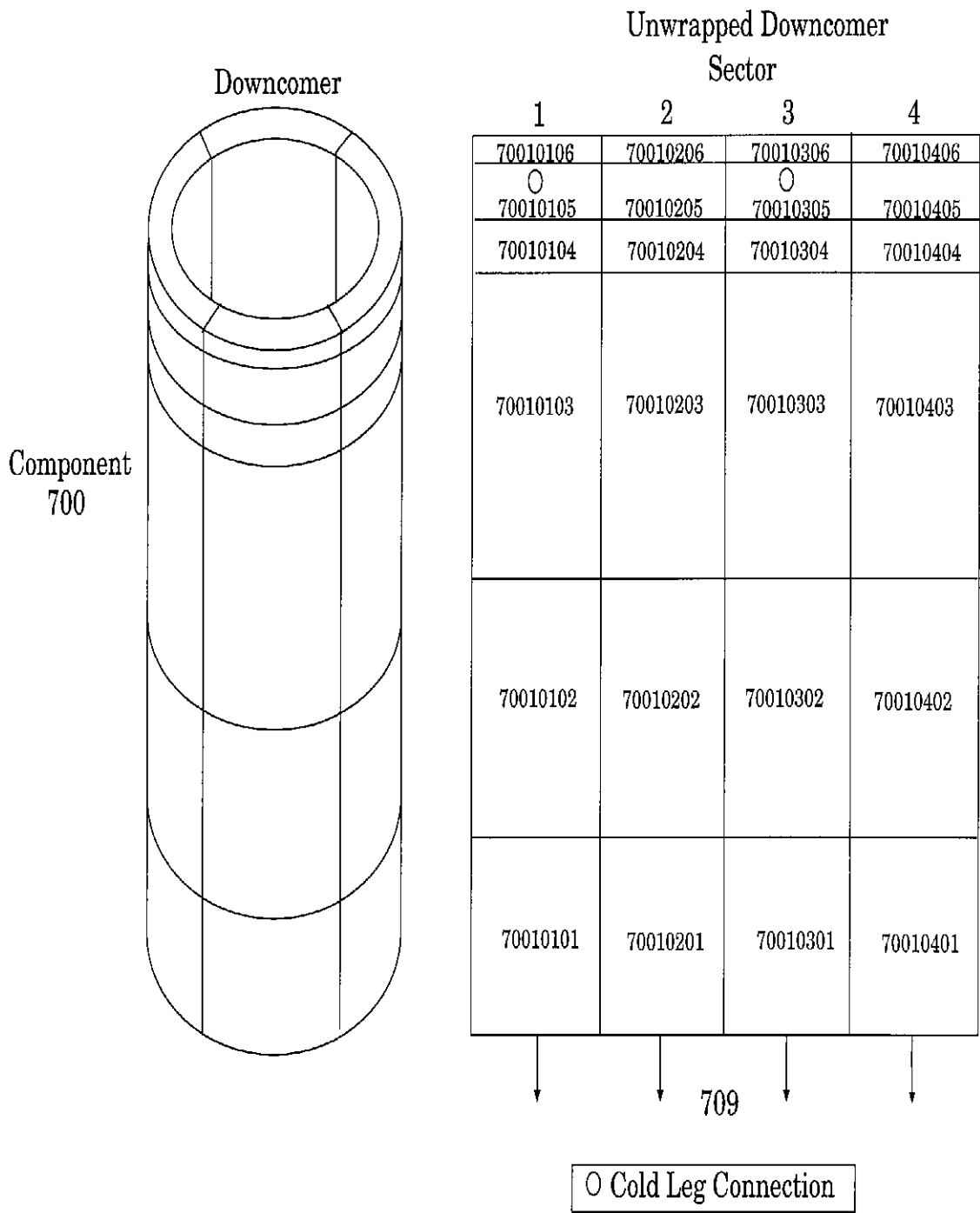


Figure 12. Nodalization of the 3D Model of the LOFT Downcomer

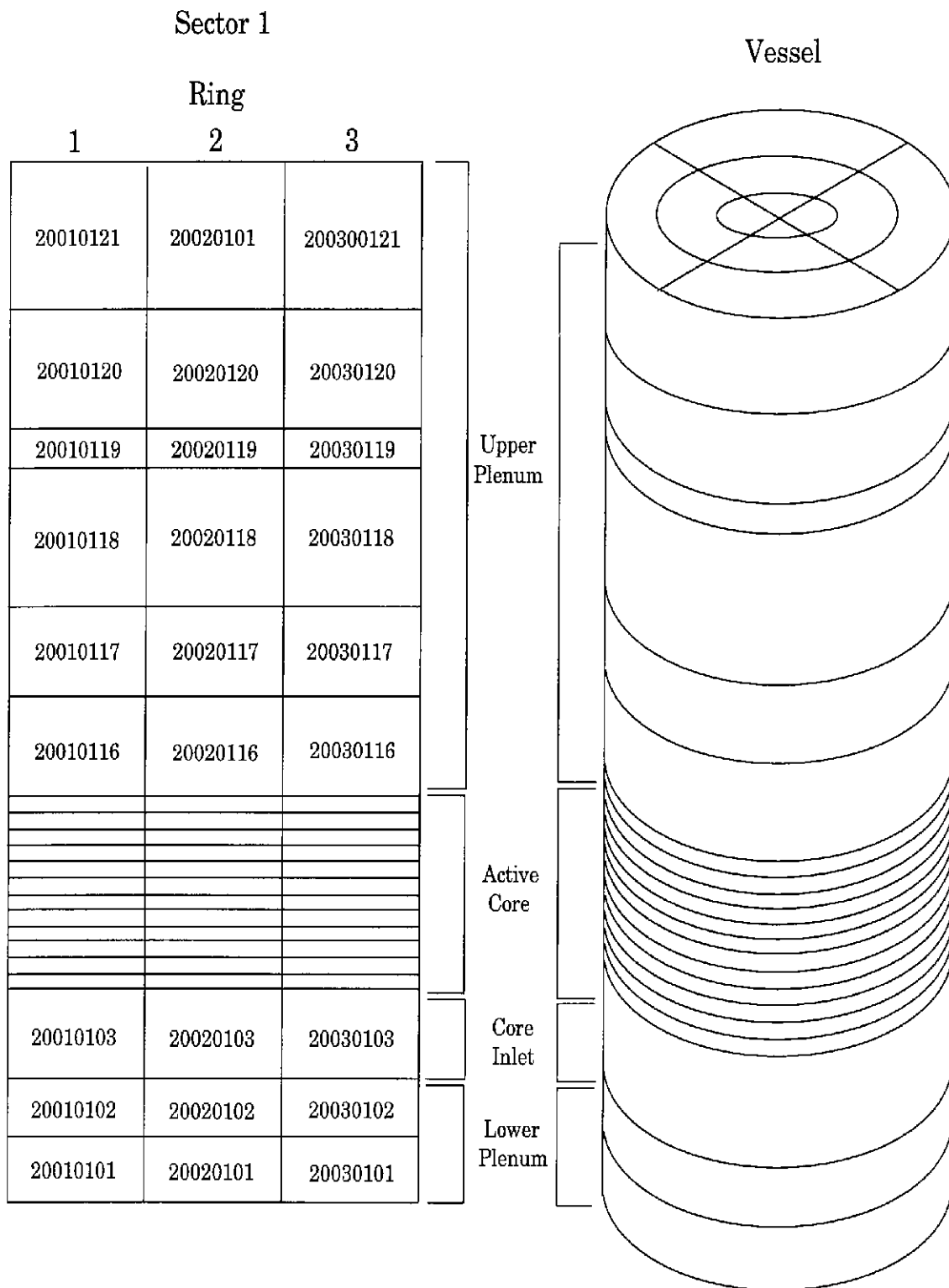


Figure 13. Nodalization of the 3D Model of the LOFT Lower Plenum, Core Inlet, Core, and Upper Plenum Regions

Steady-state calculations were performed for LOFT Test L2-5 with both the one-dimensional and three-dimensional models. Table 1 shows that the results of the steady-state calculations were in excellent agreement with the measurements.

Table 1. A comparison of calculated and measured initial conditions in LOFT Test L2-5.

Parameter	Measured Value	One-dimensional Model	Three-dimensional Model
Intact loop			
Mass flow (kg/s)	192.4 ± 7.8	192.4	192.4
Hot leg pressure (MPa)	14.94 ± 0.06	14.92	14.92
Cold leg temperature (K)	556.6 ± 4.0	556.6	556.7
Hot leg temperature (K)	589.7 ± 1.6	590.4	590.5
Pressurizer liquid level (m)	1.14 ± 0.03	1.14	1.14
Average pump speed (rad/s)	131.5 ± 1.2	130.7	130.7
Pump differential pressure (kPa)	73.3 ± 9.2	63.4	63.5
Reactor vessel			
Power (MW)	36.0 ± 1.2	36.0	36.0
Maximum linear heat generation rate (kW/m)	36.0 ± 2.7	34.3	34.3
Maximum fuel centerline temperature (K)	1660 ± 57	1710	1712
Differential pressure (kPa)	28.0 ± 1.4	28.1	28.1
Steam generator secondary side			
Pressure (MPa)	5.85 ± 0.06	5.85	5.86
Mass flow (kg/s)	19.1 ± 0.4	19.1	19.1
Feedwater temperature (K)	482.0 ± 1.2	482.0	482.0
Accumulator			
Pressure (MPa)	4.29 ± 0.06	4.29	4.29
Temperature (K)	303.2 ± 6.1	303.2	303.2
Liquid level above standpipe (m)	1.17 ± 0.01	1.16	1.16

Transient simulations of LOFT Test L2-5 were performed using the one-dimensional and three-dimensional models. Comparisons between calculated and measured results,

including the sequence of events, the overall system response, and the core thermal response, are next discussed.

The measured sequence of events for LOFT Test L2-5 is presented in Table 2. The test was initiated at 0.0 s when the quick-opening blowdown valves began to open. A reactor trip signal was generated at 0.02 s on low hot leg pressure, and the reactor scrammed shortly thereafter. The operators tripped the primary coolant pumps at 0.94 s. Flow from the accumulator, HPIS, and LPIS began at 16.8 s, 23.90 s, and 37.32 s, respectively. The accumulator emptied at 49.6 s. The fuel rod cladding temperature first departed from near the saturation temperature at 0.91 s. The peak cladding temperature occurred at 28.47 s. All of the core cladding had been quenched by 65 s, concluding the interesting portion of the test.

Table 2 also presents the calculated event times with the one-dimensional and three-dimensional RELAP5 models. The calculated event times with both RELAP5 models were generally in reasonable quantitative agreement with the measured values. One exception was that the calculated peak cladding temperatures with both models occurred near 6 s, compared to about 28 s in the test. As will be shown later, the measured cladding temperatures increased slowly between 5 s and 28 s while the calculated temperatures decreased slowly, so the effect of the difference in timing is not as significant as might be inferred from Table 2. The core cladding also quenched 10 s to 15 s earlier in the calculations than in the test.

The results of the assessment calculations are presented in the form of comparison plots, which show measured values and the corresponding calculations with the one-dimensional and three-dimensional RELAP5 models.

A comparison of calculated and measured primary system pressures is presented in Figure 14. The calculated primary system pressures were similar with both models and in reasonable agreement with the data. The measured curve contains an inflection point at about 16 s, roughly corresponding to the initiation of accumulator injection that was more pronounced than in the calculations. The calculated pressures were also slightly less than the measured values after 40 s.

Table 2. Calculated and measured sequence of events for LOFT Test L2-5.

Event	Time after rupture (s)		
	Test	One-dimensional model	Three-dimensional model
Test initiated	0.0	0.0	0.0
Reactor trip signal	0.02 ± 0.01	0.02	0.02
Quick opening blowdown valves fully opened	0.04 ± 0.01	0.04	0.04
Cladding temperatures initially deviated from saturation	0.91 ± 0.2	0.84	0.28
Primary coolant pumps tripped	0.94 ± 0.01	1.60 ¹	1.60 ¹
Subcooled break flow ended (cold leg)	3.4 ± 0.5	3.7	3.9
Steam control valve fully closed	9.38 ± 0.05	9.38	9.38
Pressurizer emptied	15.4 ± 1.0	15.5	15.5
Accumulator injection initiated	16.8 ± 0.1	15.0	14.3
HPIS injection initiated	23.90 ± 0.02	23.90	23.90
Maximum cladding temperature reached	28.47 ± 0.02	6.0	6.3
LPIS injection initiated	37.32 ± 0.02	37.32	37.32
Accumulator emptied	49.6 ± 0.1	50.0	50.5
Core cladding quenched	65 ± 2	49	55

-
1. The measured voltage and current to the pumps did not drop instantaneously to zero following the trip of the pumps in the test. Since the code assumes an instantaneous trip, the pump trip in the calculations was delayed to coincide with the measured decrease in pump speed and differential pressure.

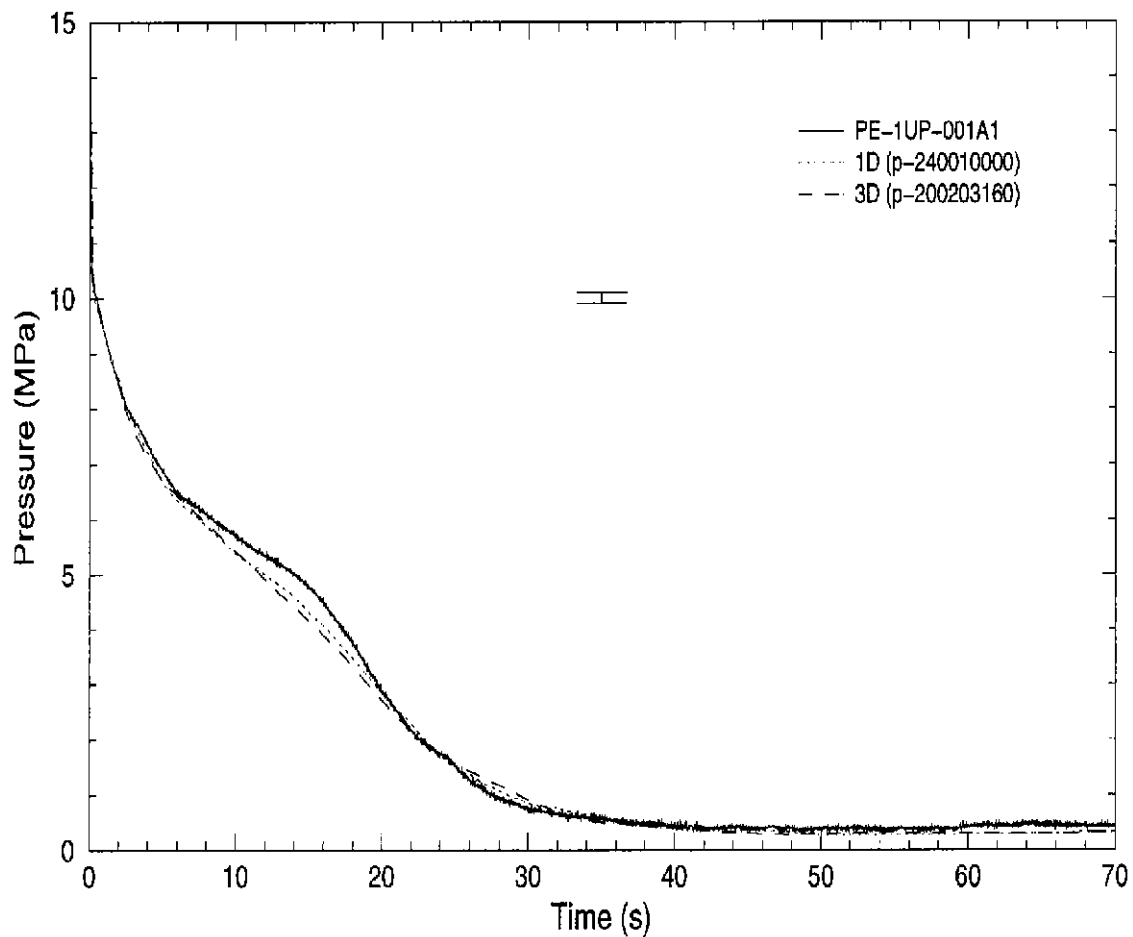


Figure 14. Calculated and measured primary system pressure for LOFT Test L2-5
 Figures 15 and 16 show calculated and measured mass flow rates in the broken loop cold leg and broken loop hot leg. The measured flow in the broken loop cold leg was substantially larger than the flow in the broken loop hot leg, particularly during the first 5 s of the transient. The fluid upstream of the cold leg break was subcooled for several seconds while the fluid upstream of the hot leg break was at the saturation temperature almost immediately after the break, leading to higher critical flow rates on the cold leg side. Both RELAP5 models predicted this trend.

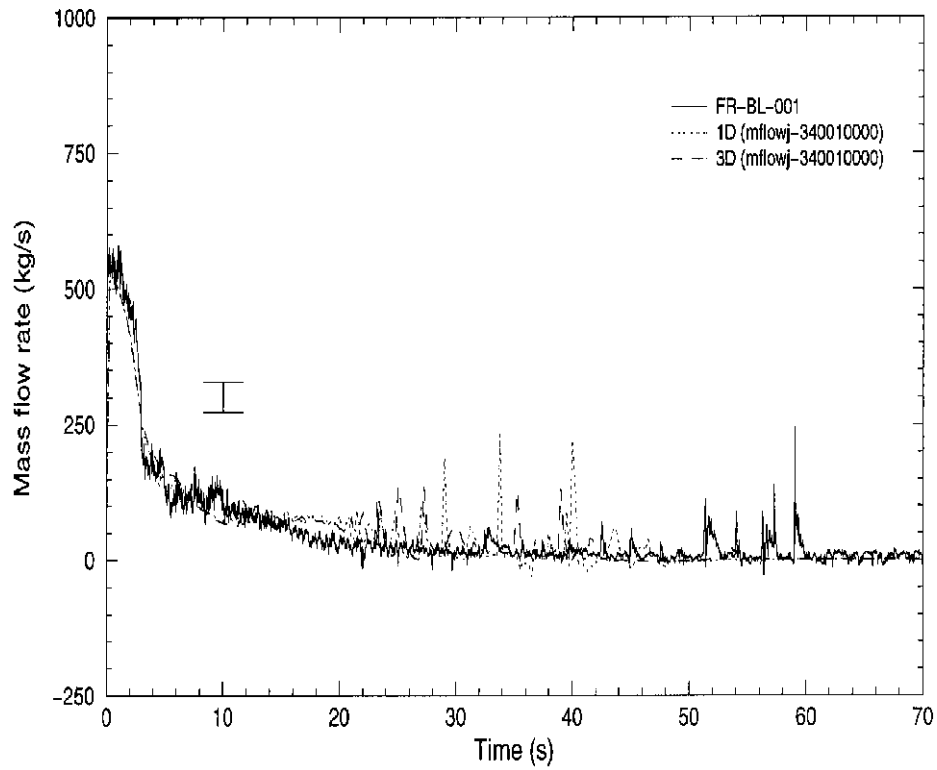


Figure 15. Calculated and measured mass flow rates in the broken loop cold leg for LOFT Test L2-5

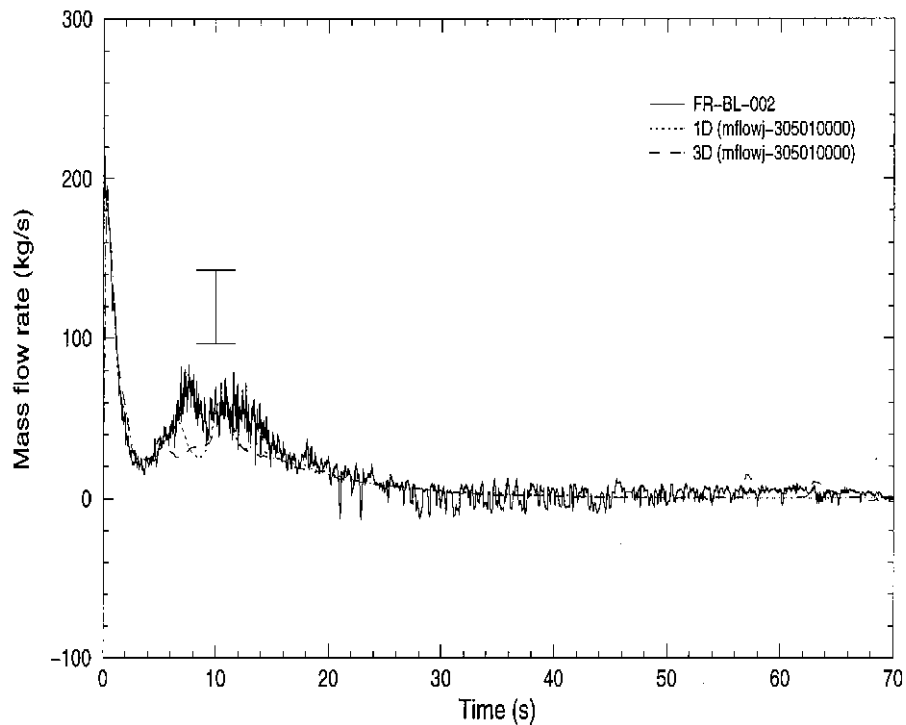


Figure 16. Calculated and measured mass flow rates in the broken loop hot leg for LOFT Test L2-5

The calculated results are generally within the uncertainty of the measurements and are thus considered to be in excellent agreement with the data.

A comparison of calculated and measured mass flow rates in the intact loop hot leg is shown in Figure 17.

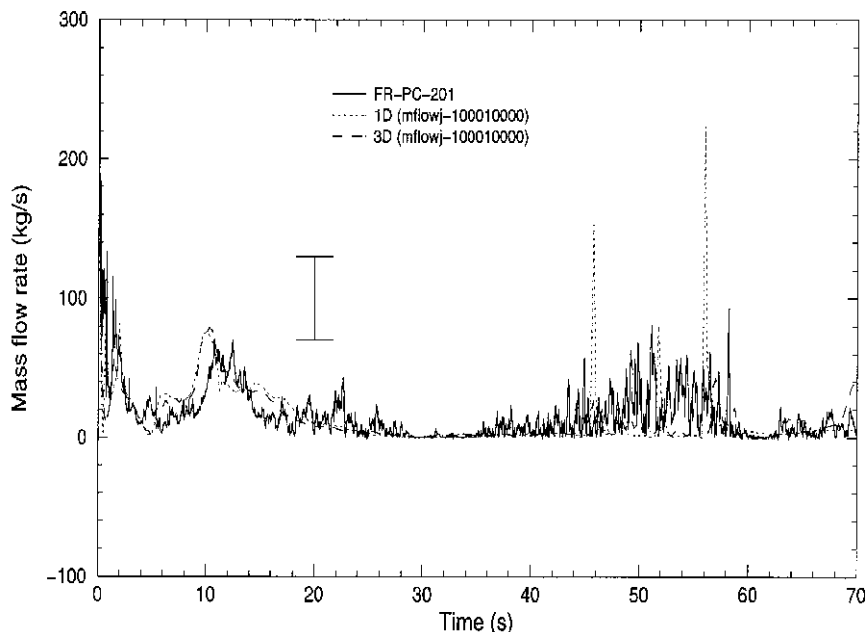


Figure 17. Absolute value of the calculated and measured mass flow rates in the intact hot leg for LOFT Test L2-5

The instrument measured only the magnitude of the flow rate and not its direction. Consequently, the absolute values of the flow rates, which are presented in Figure 17, provide a more direct indication of the agreement between the calculated and measured results. In the calculations, the flow in the hot leg was generally towards the steam generator until 5 s. The flow then reversed, going towards the reactor vessel due to the pump trip and the corresponding flow coastdown. The maximum negative flow occurred at about 10 s and was caused by vapor generation in the steam generator u-tubes, which forced flow towards the reactor vessel. The draining of the pressurizer also contributed to the flow from the hot leg to the reactor vessel. Based on the comparisons shown in Figure 17, a similar flow reversal probably occurred in the experiment. The trends in the calculations were similar to those observed in the test except that the measured results were more oscillatory, particularly between 35 s and 60 s, which roughly corresponded to the reflooding of the core.

In general, there was little difference between the results from the one-dimensional and three dimensional models insofar as loop behavior was concerned. That was not unexpected. Differences were obviously expected in the vessel.

Figure 18 presents calculated and measured fuel centerline temperatures in the central, high-powered bundle. The measured temperature decreased rapidly during the first 5 s of the transient, then remained nearly constant until 63 s, when the temperature decreased rapidly to near the saturation temperature of the fluid. The rapid temperature decrease at 63 s is referred to as a quench and indicates that the fuel rod surface had been wetted by the advancing mixture level during the reflooding of the core. The calculated temperatures were similar to the measurement except that the quench occurred earlier than in the test, particularly in the calculation with the one-dimensional model, and both calculated temperatures decreased at a faster rate than in the test between 5 s and the quench time.

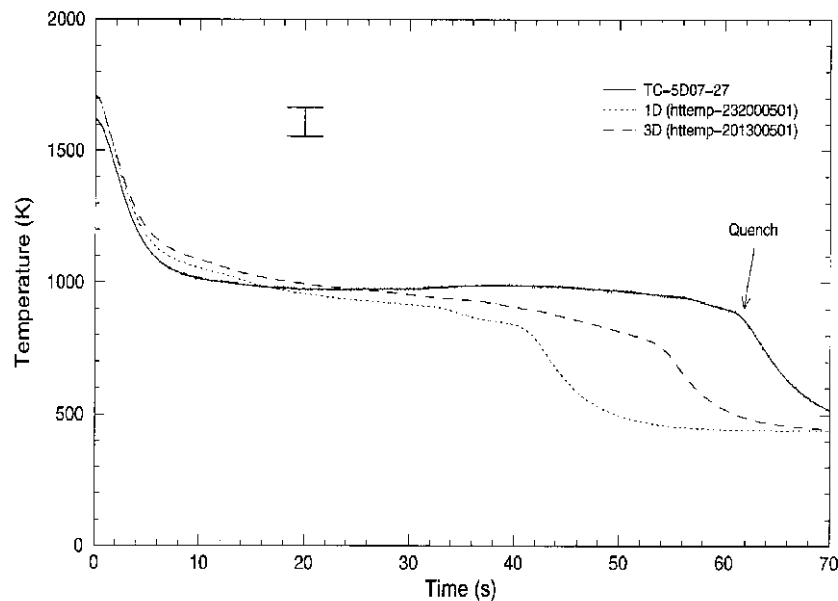


Figure 18. Calculated and measured fuel centerline temperatures in ring 1, sector 3, level 8 for LOFT Test L2-5

Comparisons between calculated and measured cladding temperatures as a function of elevation are presented in Figures 19, 20, and 21. The results correspond to axial levels 6, 7, and 8 of ring 1, sector 2 of the three-dimensional model. Ring 1 represents most of the central, high-powered fuel rod bundle, and sector 2 represents the quadrant connected to the broken loop hot leg. The one- and three-dimensional models produced similar results, underpredicting the peak cladding temperature and quenching earlier than in the experiment. However, quenching behavior in the three-dimensional model more closely matched the data. This is mainly attributed to the fact that the high-powered fuel rods were attached to a relatively hot fluid channel in the three-dimensional model whereas the high-powered fuel rods were attached to a single, average channel in the one-dimensional model.

Significant radial variations in cladding temperatures were observed in both the test and the calculation with the three-dimensional model as shown in Figures 22 and 23. Figure 22 shows measured temperatures in rings 1 through 3 at level 9. The thermocouples referred to in the figures were all located at the same elevation and within the same sector so that the measured differences in results were due to radial effects. Figure 23 shows the corresponding calculated results with the three-dimensional model. The calculated and measured temperatures both show the influence of the radial power profile, with the highest temperatures in ring 1, the high-powered ring, and the lowest temperatures in ring 3, the low-powered ring. The radial variation in cladding temperatures was more pronounced in the test than in the calculation, primarily because the time of CHF varied more in the test.

The hydraulic responses of the primary and secondary coolant systems calculated with RELAP5-3D[®] and the three-dimensional input model were generally in reasonable agreement with LOFT Test L2-5. The results were generally as good as or better than the results obtained using the RELAP5/MOD3 or RELAP5-3D[®] one-dimensional models. The calculated thermal response of the core fuel rods with the three-dimensional model was also generally similar to that observed in the test. The calculated peak cladding temperature was 990 K while the measured peak cladding temperature was 1078 K. The

most significant deviations between the calculated and measured thermal responses were that the calculated peak cladding temperature occurred earlier than in the test and that the top-down rewet that was observed near 15 s in the test was not predicted.

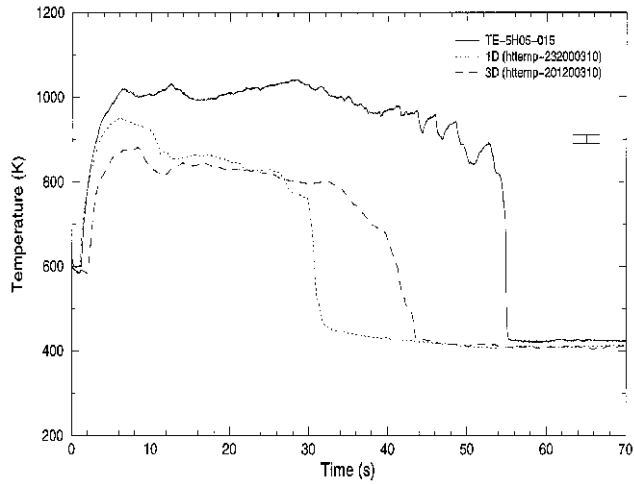


Figure 19. Calculated and measured cladding temperatures in ring 1, sector 2, level 6 for LOFT Test L2-5

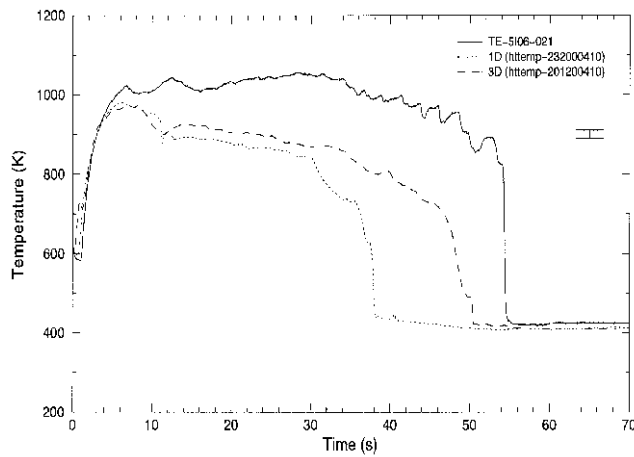


Figure 20. Calculated and measured cladding temperatures in ring 1, sector 2, level 7 for LOFT Test L2-5

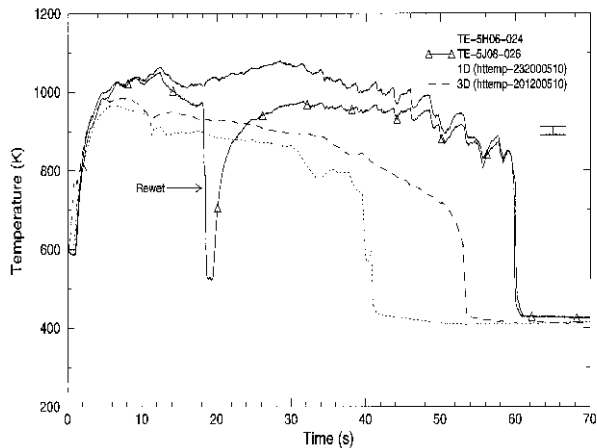


Figure 21. Calculated and measured cladding temperatures in ring 1, sector 2, level 8 for LOFT Test L2-5

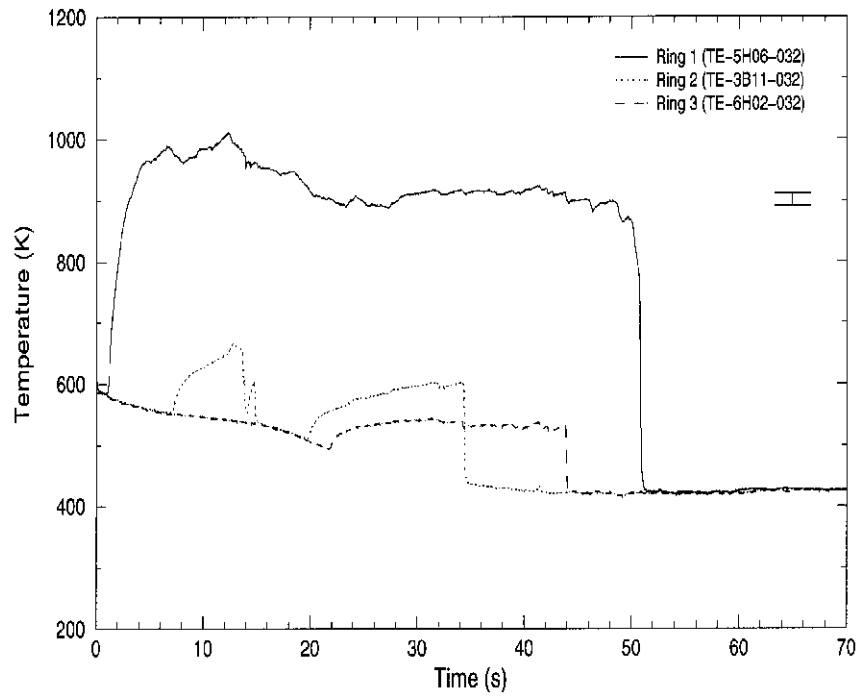


Figure 22. Measured cladding temperatures showing radial effects in sector 2, level 9 for LOFT Test L2-5

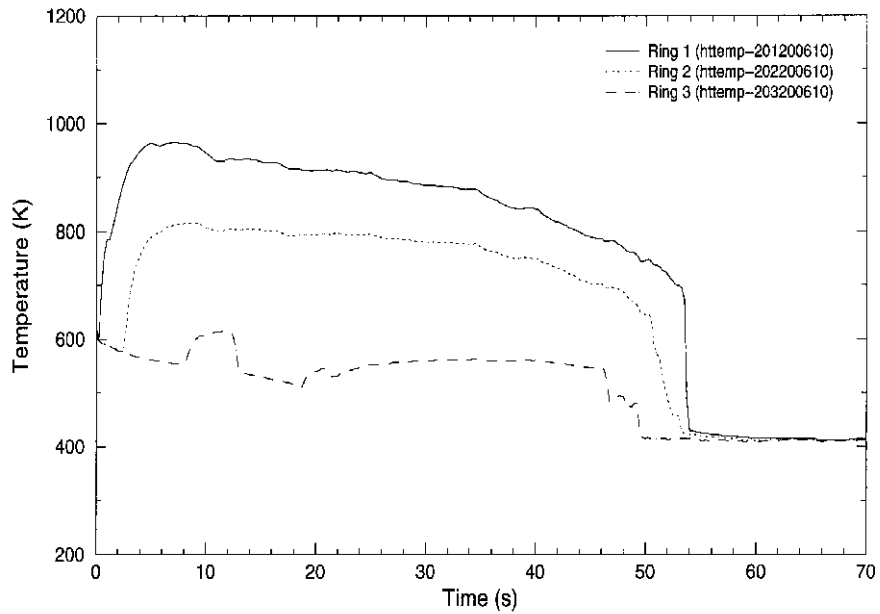


Figure 23. Calculated cladding temperatures showing radial effects in sector 2, level 9 for LOFT Test L2-5

Multi-Dimensional Neutron Kinetics Model

The multi-dimensional neutron kinetics model in RELAP5-3D is based on the NESTLE¹⁴ code developed by Paul Turinsky and co-workers at North Carolina State University under an INEEL initiative. The NESTLE code solves the two or four group neutron diffusion equations in either Cartesian or hexagonal geometry using the nodal expansion method. Three, two, or one dimensional models may be used. Several different core symmetry options are available including quarter, half, and full core options for Cartesian geometry and 1/6, 1/3, and full core options for hexagonal geometry. Zero flux, non-reentrant current, reflective, and cyclic boundary conditions are available. The steady-state eigenvalue and time dependent neutron flux problems can be solved by the NESTLE code as implemented in RELAP5-3D.

The few group neutron equations are spatially discretized using the Nodal Expansion Method (NEM). Quartic or quadratic polynomial expansions are used for the transversely integrated fluxes in the Cartesian and hexagonal geometries respectively. Discontinuity factors are used to correct for homogenization errors.

Transient problems employ a user-specified number of delayed neutron precursor groups. The time discretization is done with a fully implicit method. The delayed neutron precursor equations are integrated analytically assuming a linear variation of the neutron flux.

An outer-inner iteration strategy is employed to solve the matrix of equations resulting from the temporal and spatial discretization. Outer iterations use Chebyshev acceleration. Inner iterations use a point or line SOR iteration scheme. The non-linear iterative strategy associated with the NEM is employed. Using the non-linear iterative strategy means that the system of equations is equivalent to the finite difference method using the box scheme. This means that the code can solve either the nodal or finite difference representation of the few-group neutron diffusion equations.

Thermal-hydraulic (TH) feedback is accomplished through the neutron cross sections. The thermal-hydraulic conditions in the neutron kinetics nodes are computed by RELAP5-3D using the hydraulic model of the system specified by the user using normal RELAP5 input. The conditions in the RELAP5 volumes are mapped onto the kinetics nodes by map functions using user-supplied data. The neutron cross sections in the kinetics nodes are computed from RELAP5 calculated TH conditions and user supplied composition data. The cross section model is quite general and the user can choose between different sets of TH conditions for use in the neutron cross section model, e.g., either void fraction or coolant density as one of the independent variables in the cross section model. Neutron cross sections are computed for each kinetics node from the TH conditions mapped onto the individual nodes and the composition data mapped onto the same nodes.

The compositions are mapped onto the kinetic nodes using user supplied composition maps. In this way a small number of compositions and a small number of RELAP5 volumes and heat structures may be mapped to a large number of kinetics solution nodes. Discontinuity factors are modeled using the neutron cross section model so that they may change as the TH conditions in the kinetics nodes change during the course of the transient.

A control rod model has been implemented and each neutron kinetics node may contain any number of control rods. Control rods may be inserted from either the top or bottom of the reactor. The control rods may be grouped into banks, with the banks having the same insertion depth and velocity. The position of a control rod bank can also be determined from a control variable or a general table. Scram signals may be initiated by RELAP5 trips.

The reactor power and its distribution computed by the kinetics module are supplied to the RELAP5 TH solution through the same maps that are used to compute the neutron cross sections. As the neutron flux and its distributions change during the course of the transient, so does the power supplied to the individual RELAP5 volumes and heat structures change accordingly.

The decay heat model as implemented in previous code versions for the point kinetics is used to compute the decay heat in the multi-dimensional neutron kinetics model. The decay heat is calculated in each kinetics node based on the fission power in that node.

Verification

The implementation of the NESTLE neutron kinetics has been verified by the simulation of the NEACRP¹⁵ three dimensional benchmark problems¹⁶. A series of three PWR rod ejection accidents from Hot Zero Power and Hot Full Power were proposed as a benchmark by the NEACRP. Series A, the ejection of a central rod, and series B, the ejection of peripheral rods, were chosen for simulation using the spatial kinetics option. The location of the ejected control rods and the initial core configuration are shown in Figure 24. For the series A and B transients one-quarter geometry was adequate.

The RELAP5 core model for the benchmark problem consisted of a sequence of parallel pipes as shown in Figure 25. Each pipe was described using a series of heat structures and control volumes to model the fuel and coolant from a single assembly. A separate inlet reservoir was provided for each pipe and was set at a constant pressure, temperature, and boron concentration. Each pipe was connected to its reservoir using a time-dependent junction that provided identical, constant flow to each assembly. The outlet of each pipe was connected to an outlet reservoir using a series of branches. Since a maximum of nine junctions per branch is allowed, additional branches were used to accommodate the total of 47 pipes of the quarter core model.

During the course of the analysis, various thermal-hydraulic mesh structures were examined. The finest axial mesh used for the pipes corresponds to that prescribed in the NEACRP problem with the exception that the three smallest nodes at the bottom and top of the core were combined into a single thermal- hydraulic node. The original NEACRP mesh structure for the neutronic solution was retained. This provided for a total of 14 axial thermal-hydraulic meshes in each pipe. For purposes of the thermal-hydraulic calculation, the reflector was modeled as a separate, single pipe because of the very small temperature rise anticipated in the reflector.

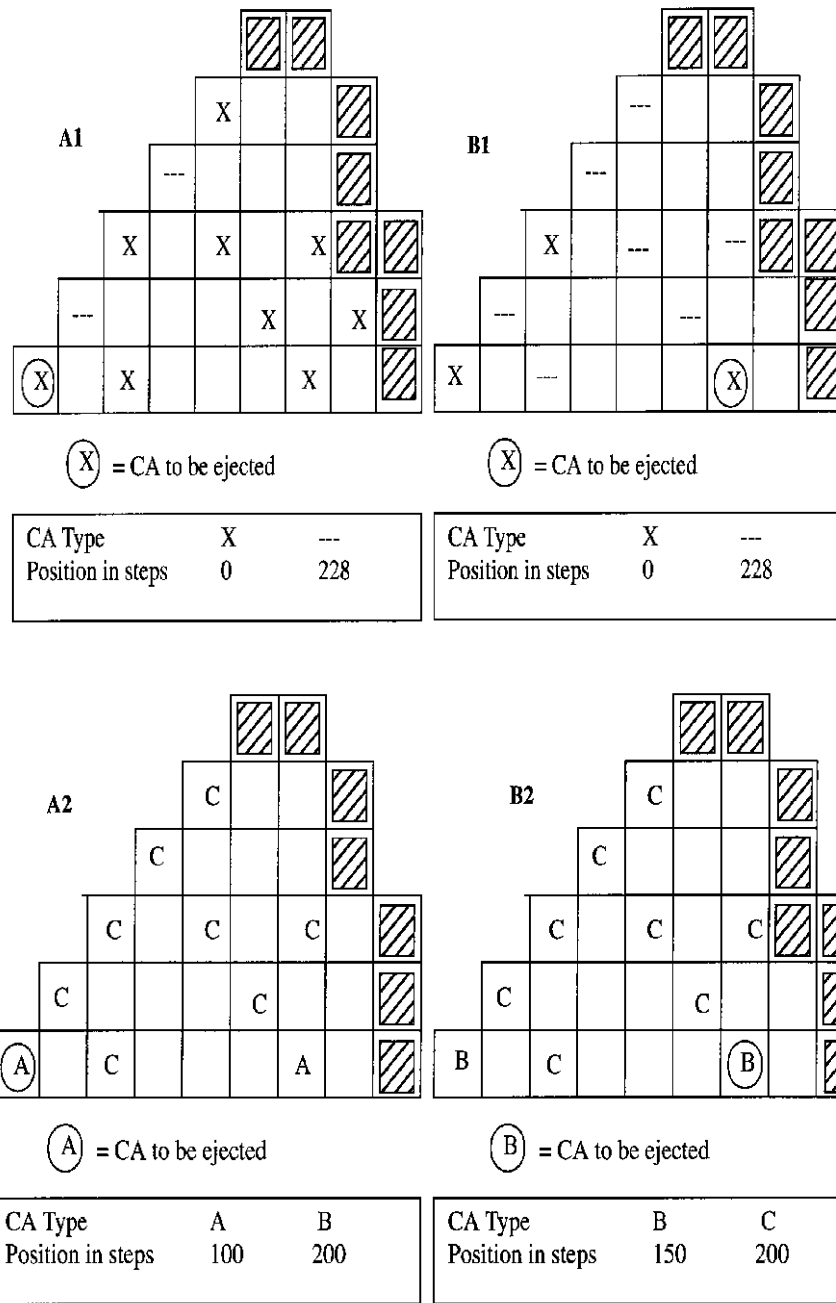


Figure 24. Initial Core Configuration for Series A and B Rod Ejection Transients For the fuel pin model 8, 1, and 2 meshes in the fuel pellet, gap, and cladding, respectively, were used. In order to generate an effective Doppler temperature in RELAP5 consistent with that prescribed in the NEACRP problem,

$$T = (1 - \alpha)T_{F,C} + \alpha T_{F,S}$$

a very small central and peripheral fuel pellet mesh was used such that the area of these regions corresponds to the weighting of the surface temperature, $T_{F,S}$, and centerline fuel temperature, $T_{F,C}$ specified in the benchmark problem. All other fuel pellet meshes were equidistant.

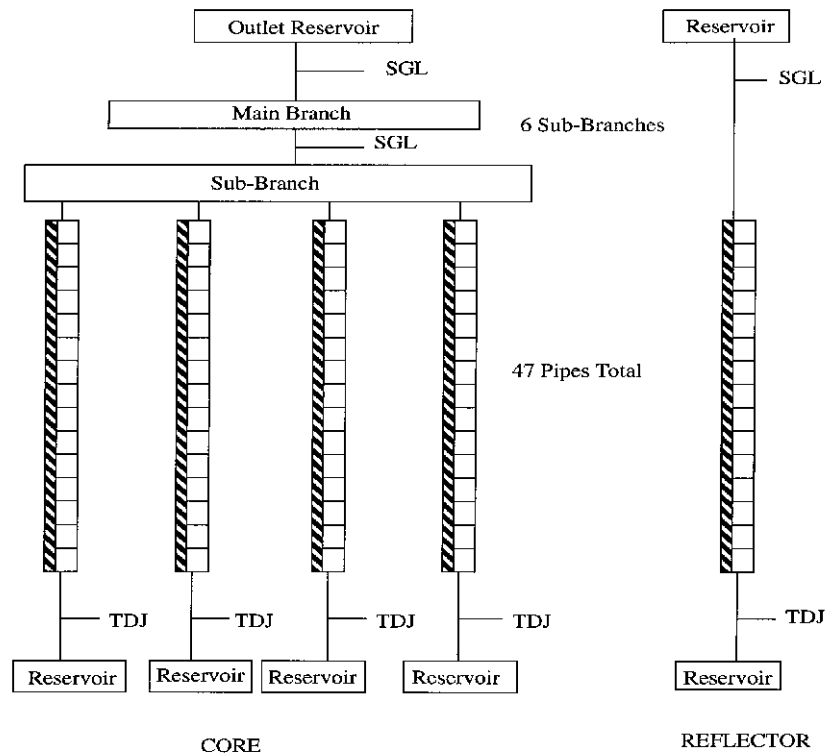


Figure 25. RELAP5-3D Core Nodalization for Test Problem

Because the benchmark problem specifies gap conductance and RELAP5 only accepts gap conductivity, the following relation was used:

$$k = h\Delta r$$

where k and h are the gap conductivity and conductance, respectively, and Δr is the gap width. This expression is valid for a small gap width as used in the benchmark problem.

The axial mesh structure used for the neutronic solution was identical to that specified in the benchmark problem and four nodes per fuel assembly were used in the radial plane. The partial cross sections prescribed in the NEACRP benchmark were processed into an equivalent set of cross section multipliers to coincide with the modeling used in RELAP5. Some minor discrepancy persisted since it is not possible to construct a completely consistent set of partial cross section data for the diffusion coefficient used in RELAP5 based on the partial transport cross section data specified in the benchmark problem.

The steady state solution was obtained by running a null transient with RELAP5 for 20 seconds using time steps of 0.05 secs. The current algorithm provides for a thermal-hydraulics update only at the completion of each k-effective solution. The convergence criteria for the neutronic solution were set at 10^{-4} and 10^{-5} for the global fission source and k-effective, respectively. The coupling coefficients in the NEM nonlinear iteration method were updated every five outer iterations. For the transient solution, the global fission source convergence criterion was increased to 10^{-5} . The time step sizes for the transients are given in Table 3.

Table 3. Time Step Sizes Used in the Analyses

Case	0 to 1 second	1 to 5 seconds
Zero Power (A1,B1)	0.001	0.01
Full Power (A2,B2)	0.01	0.05

The results of the four transient cases are summarized in Table 4. For each of the four cases the predicted values and their deviations from the reference are shown. The reference results are those reported at the Karlsruhe conference¹⁷. The transient power for each of the four cases is compared with the reference in Figure 26 for A1 and B1 and in Figure 27 for A2 and B2. The RELAP5 radial power distribution at axial plane 6 (out of 16) for problem A1 is compared to the reference in Figure 28 for the steady state (t=0), for the maximum power condition (t=0.611 secs.), and for the asymptotic core state (t=5 secs.).

Table 4. Summary of the RELAP5 NEACRP Benchmark Calculation Results

	A1		B1		A2		B2	
Steady State								
Critical Boron Conc. (ppm)	563.4	-4.6	1253	-1.4	1154	-6.8	1183	-4.8
Assembly Peaking Factor	2.865	0.3%	1.926	-0.2%	2.203	-0.8%	2.101	-0.4%
Max. Fuel Temp. (deg. C)	286.0	0.0%	286.0	0.0%	1612	-3.6%	1528	-3.1%
Rod Worth (pcm)	820	-0.2%	836	0.6%	91	1.7%	99	-0.1%
@ Time of Maximum Power								
Time (sec)	0.611	0.046	0.519	0.004	0.100	-0.020	0.110	-0.010
Relative Core Power	0.911	-22%	2.252	-7.8%	1.085	0.5%	1.063	0.0%
Maximum Fuel Temp. (deg. C)	337.2	-2.3%	325.5	-0.9%	1613	-3.5%	1528	-3.1%
@ Time = 5 sec								
Relative Core Power	0.191	-2.2%	0.317	-1.1%	1.036	0.0%	1.038	0.0%
Max. Fuel Temp. (deg C)	650.0	-3.2%	549.9	-1.5%	1632	-3.5%	1539	-3.1%

As indicated in Table 4, the RELAP5 steady state results for the hot zero power cases are in reasonably good agreement with the reference results. RELAP5 does show a slight negative bias in the prediction of the critical boron concentration for both cases A1 and B1. Also note that RELAP5 is consistently lower than the reference in its prediction of the power in the rodded locations for the steady-state. This is consistent with the negative bias in the critical boron prediction since a greater estimation of the total rod worth would lead to a lower critical boron concentration. The negative bias is larger in case A1 because there are several more rods inserted than in case B1.

The RELAP5 ejected rod worth prediction for both cases is in good agreement with the reference result. As shown in Figure 26, agreement of the transient results is excellent for case B1, however, discrepancies exist in the RELAP5 and reference results for case A1. RELAP5 predicts the maximum power will occur 0.046 seconds later and have a magnitude 22.1% lower than the reference calculation.

The asymptotic core state predicted by RELAP5 is in reasonably good agreement with the reference result as shown in Table 4, although RELAP5 shows a slight negative bias in the asymptotic core power.

The RELAP5 steady state results for the hot full power cases show a slight negative bias in the prediction of the critical boron concentration.

As shown in Figure 27, the RELAP5 transient results for case A2 shows a positive bias in the prediction of the maximum power, whereas case B2 is in close agreement with the reference results. As shown in Table 4, there is good agreement between RELAP5 and the reference in the prediction of the time of the maximum power, as well as in the prediction of the asymptotic core power.

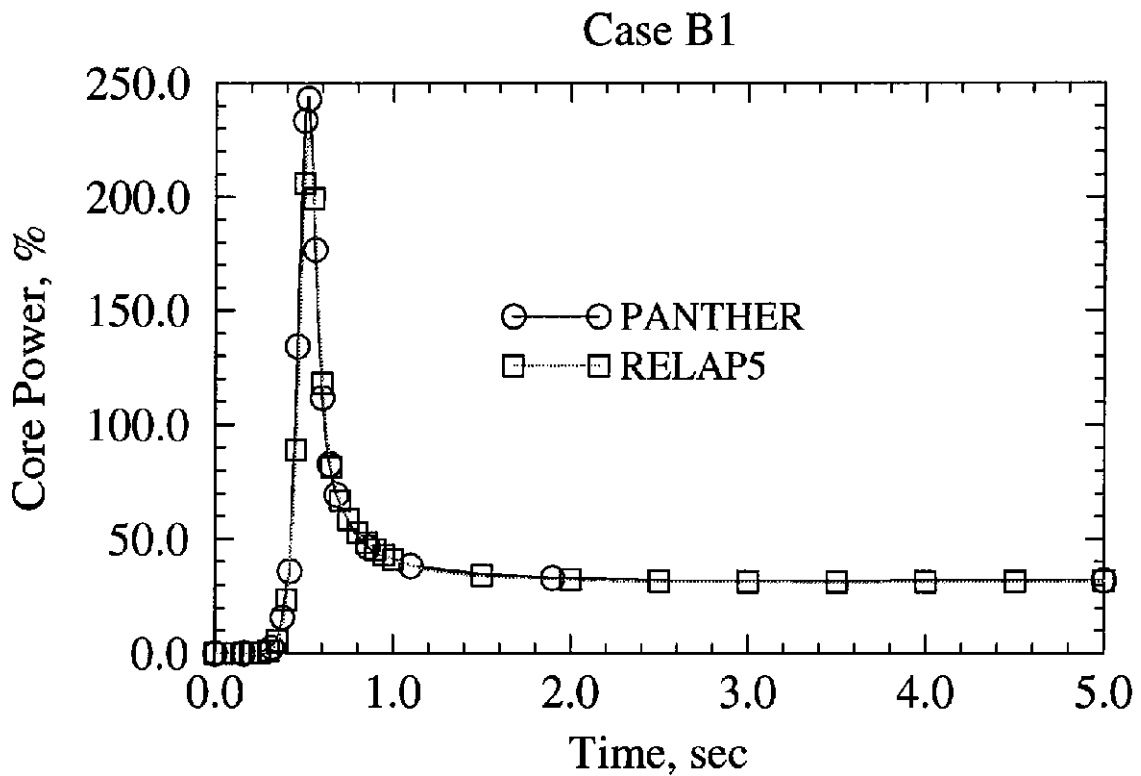
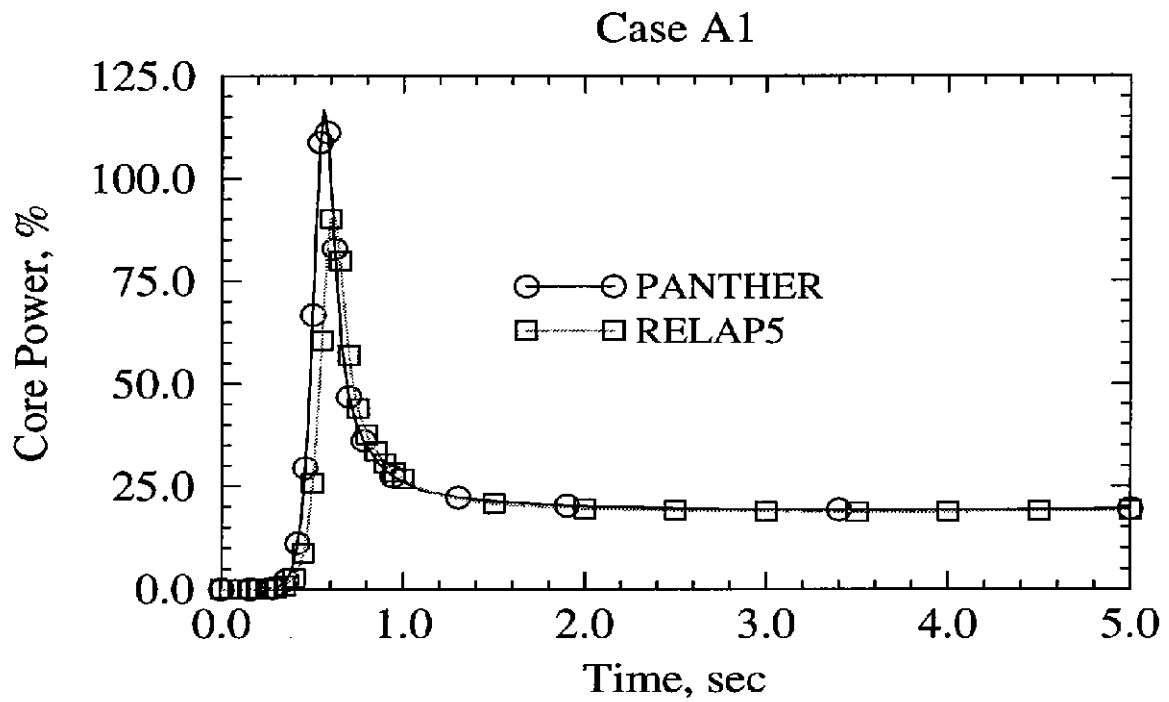


Figure 26. Transient Core Power for Rod Ejection from Hot Zero Power

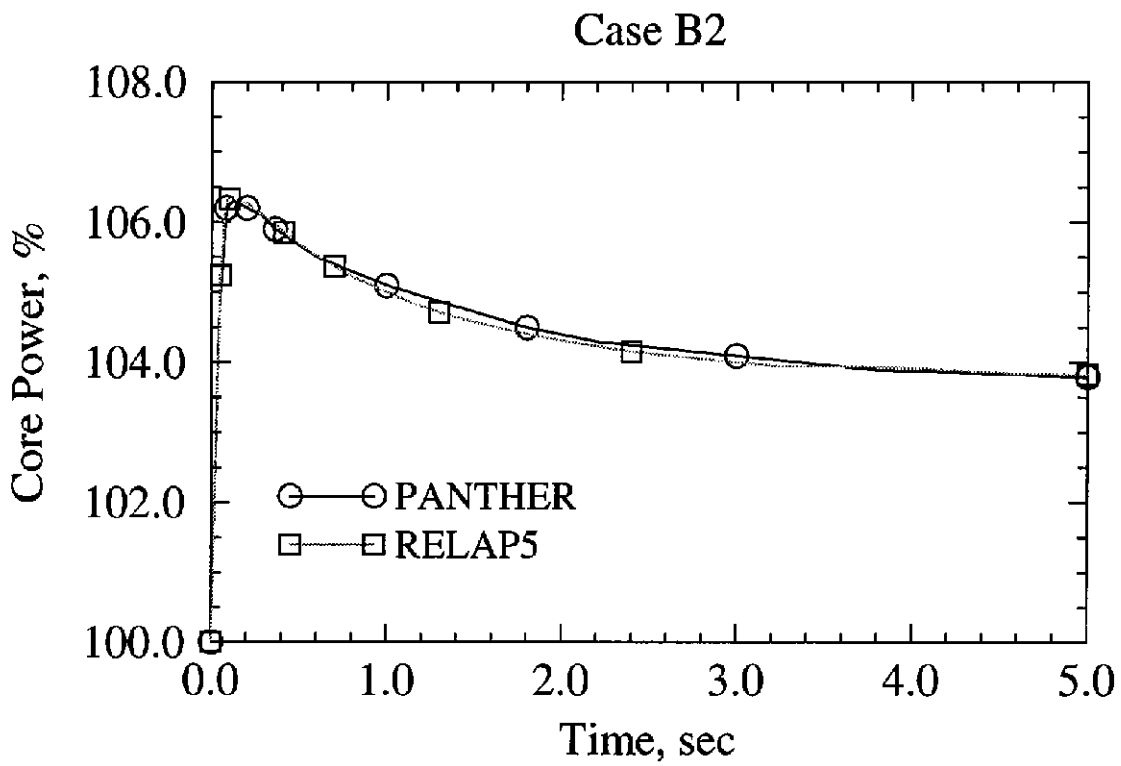
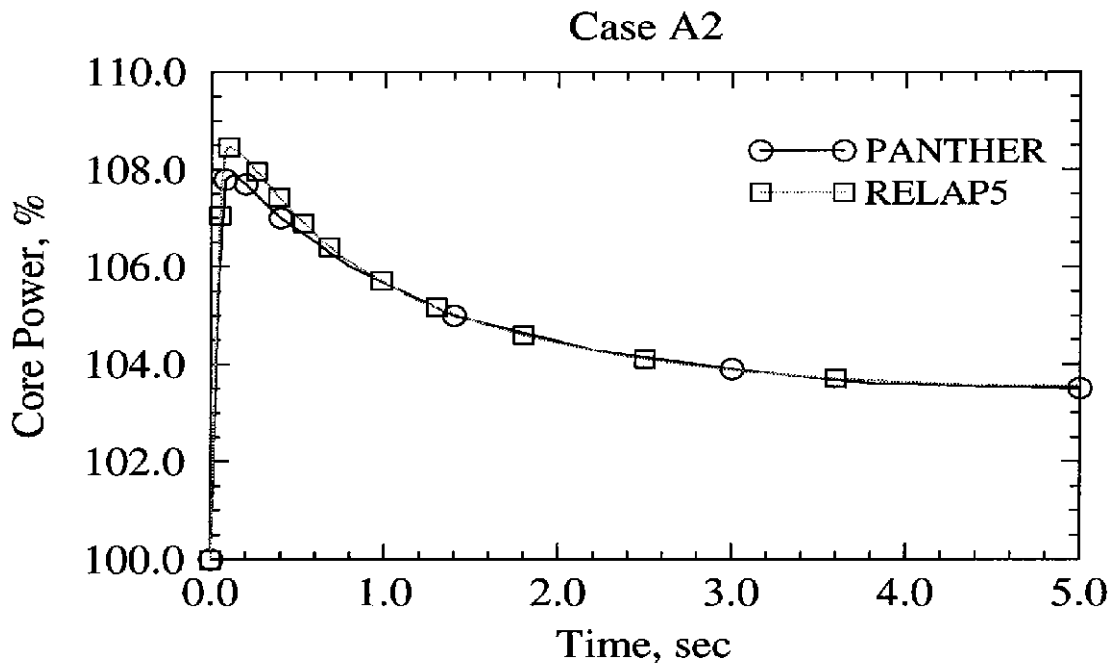


Figure 27. Transient Core Power for Rod Ejection from Hot Full Power

Steady-State								
5	PAN				0.293	0.354		
	REL				0.286	0.359		
	% D				-2.4	1.4		
6				0.752	0.533	0.497	0.285	
				0.753	0.534	0.501	0.290	
				0.1	0.2	0.8	1.8	
7			0.545	0.757	0.393	0.380	0.206	
			0.529	0.757	0.382	0.382	0.202	
			-2.9	0.0	-2.8	0.5	-1.9	
8		0.964	0.867	1.000	0.745	0.301	0.294	0.226
		0.964	0.867	1.000	0.745	0.292	0.296	0.230
		0.0	0.0	0.0	0.0	-3.0	0.7	1.8
9	0.533	0.793	0.575	0.945	0.951	0.527	0.214	0.285
	0.516	0.792	0.557	0.943	0.951	0.528	0.209	0.289
	-3.2	-0.1	-3.1	-0.2	0.0	0.2	-2.3	1.4
	I	J	K	L	M	N	O	P
At Time of Maximum Power								
5	PAN				0.128	0.150		
	REL				0.125	0.151		
	% D				-2.3	0.7		
6				0.362	0.242	0.214	0.120	
				0.362	0.242	0.214	0.121	
				0.0	0.0	0.0	0.8	
7			0.316	0.390	0.188	0.169	0.088	
			0.307	0.390	0.183	0.170	0.086	
			-2.8	0.0	-2.7	0.6	-2.3	
8		0.790	0.562	0.540	0.371	0.140	0.126	0.093
		0.790	0.561	0.540	0.370	0.136	0.127	0.094
		0.0	-0.2	0.0	-0.3	-2.9	0.8	1.1
9	1.000	0.778	0.390	0.513	0.474	0.248	0.093	0.117
	1.000	0.777	0.378	0.513	0.474	0.248	0.090	0.118
	0.0	-0.1	-3.1	0.0	0.0	0.0	-3.2	0.9
	I	J	K	L	M	N	O	P
At Final Time t = 5 seconds								
5	PAN				0.143	0.168		
	REL				0.140	0.172		
	% D				-2.1	2.4		
6				0.392	0.266	0.239	0.135	
				0.393	0.268	0.241	0.138	
				0.3	0.8	0.8	2.2	
7			0.333	0.417	0.205	0.188	0.099	
			0.323	0.418	0.199	0.189	0.097	
			-3.0	0.2	-2.9	0.5	-2.0	
8		0.802	0.581	0.569	0.397	0.153	0.142	0.106
		0.802	0.581	0.570	0.398	0.149	0.143	0.108
		0.0	0.0	0.2	0.3	-2.6	0.7	1.9
9	1.000	0.785	0.403	0.540	0.505	0.269	0.104	0.134
	1.000	0.785	0.391	0.541	0.506	0.271	0.102	0.136
	0.0	0.0	-3.0	0.2	0.2	0.7	-1.9	1.5
	I	J	K	L	M	N	O	P

Figure 28. Core Radial Power Distribution at Axial Plane 6 for Case A1

BPLU Matrix Solver

The Border Profiled Lower Upper (BPLU) matrix solver is used to efficiently solve sparse linear systems of the form $AX = B$. BPLU is designed to take advantage of pipelines, vector hardware, and shared-memory parallel architecture to run fast. BPLU is most efficient for solving systems that correspond to networks, such as pipes, but is efficient for any system that it can permute into border-banded form.

Speed-ups are achieved for RELAP5-3D[®] running with BPLU over the default solver. For almost one-dimensional problems, there is no speed-up; however, for problems with wider bandwidths, especially those with three-dimensional regions, significant speed-ups may be achieved. One of the standard installation problems, “3dflown.i” illustrates the reduction in run time that can be achieved. The problem is a simple cube subdivided into a 3x3 region in each of the Cartesian coordinate directions (Figure 29). There are nine cases examined with this model, comprised of flow in each coordinate direction (x,y,z) of vapor only, liquid only, and a two-phase mixture.

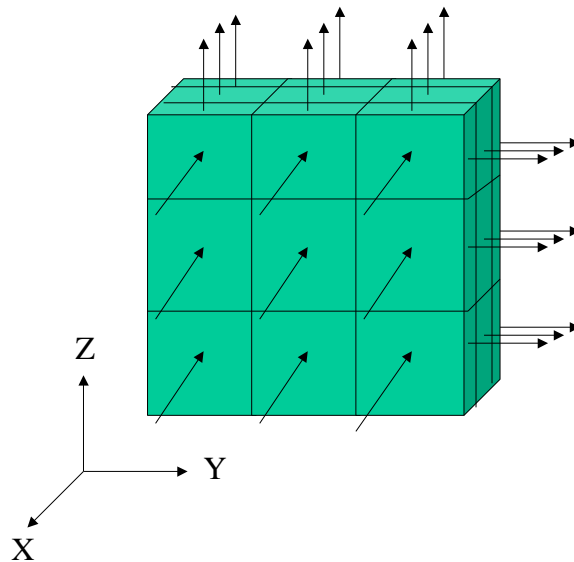


Figure 29. 3dflow problem

Table 5 compares the CPU times required for the nine cases for the default solver and the BPLU solver. Results show an average reduction in CPU time of 63%.

Table 5. Comparison of Run Times for 3dflown.i Using Default and BPLU Solvers

Case	Default Solver (CPU secs.)	BPLU Solver (CPU secs.)	Ratio
1	7.179600	2.437199	2.94584
2	7.142498	2.110301	3.38459
3	6.903399	2.718000	2.53988
4	6.141501	2.421701	2.53603
5	5.512910	2.117097	2.60399
6	5.817507	2.698403	2.15591
7	6.166502	2.432401	2.53515
8	7.405095	2.116199	3.49924
9	6.396306	2.696500	2.37208

The BPLU algorithm is designed to solve “nearly-banded” coefficient matrices directly. It is a variation of banded Gaussian Elimination with partial pivoting that incorporates variable reordering. A nearly-banded matrix is a sparse matrix that can be written as the sum of a banded matrix and a matrix of outriggers or non-zero entries that lie outside the band. The algorithm restructures the linear system into a form that can be solved efficiently on a vector-parallel computer, does not waste operations on zero entries, and controls the creation of non-zero elements.

The algorithm is suitable for and has been tested with the linear systems of the following variety: the RELAP5 semi-implicit time step matrix, the RELAP5 nearly-implicit time step matrix, and the NEWEDGE field equations matrix. All these matrices are nearly banded with outriggers. Further, the structure of the nearly-implicit matrix is similar to that of the semi-implicit matrix, but with the elements replaced by 2x2 blocks of elements. The NEWEDGE matrix replaces the 2x2 blocks with 5x5 blocks.

Two considerations lead to further efficiencies. First, the block structure discussed above leads to a profile rather than a solid band structure for which zero operations can be avoided by using a variable row length during row reduction. Profiled-structures also arise from connectivity relationships among the variates. Therefore, the BPLU algorithm uses a profile, rather than a banded, solver. Second, a nearly-banded matrix can frequently be decomposed into the sum of a banded and an outrigger matrix in more than one way. Selection of the bandwidth for the decomposition is tied to reducing the amount of work associated with solving the reorganized system.

OTHER IMPROVEMENTS IN RELAP5-3D

Other improvements in the RELAP5-3D code include:

- More accurate water properties derived from the National Bureau of Standards and National Research Council
- Enhanced robustness from intelligent recovery from advancement failure
- Graphical User Interface (beta-test)
- More implicit momentum equation permitting larger time step sizes
- Multidimensional heat conduction model for modeling graphite structures in RBMK reactors
- Windows '95/98/NT version

Ongoing and planned DOE funding will provide additional improvements:

- Ability to couple to other codes (e.g. CFD)
- Random-access plot/restart file
 - Fuel swelling model

RELAP5-3D AVAILABILITY

The INEEL will make the RELAP5-3D code available to domestic and international organizations that join the International RELAP5 Users Group (IRUG). This is a subscriber-funded group that takes part in guiding the future development and maintenance of the code. Organizations interested in obtaining the code will be given the opportunity to participate at one of two levels:

- Participant - Organizations that wish to receive the code, future updates, and some on-call assistance.
- Member - Organizations that wish to receive the code, future updates, a guaranteed level of on-call assistance, and participate in voting on improvements.

Both domestic (U.S.) and non-domestic organizations may choose between these two levels of participation. More information on joining IRUG can be found at <http://www.inel.gov/relap5/irug.htm>.

REFERENCES

1. J. A. Findley and G. L. Sozzi, "BWR Refill-Reflood Program – Model Qualification Task Plan," EPRI NP-1527, NUREG/CR-1899, GEAP-24898, October 1981.
2. T. M. Anklam, R. J. Miller, M. D. White, "Experimental Investigation of Uncovered-Bundle Heat Transfer and Two-Phase Mixture Level Swell Under High-Pressure and Low Heat Flux Conditions," NUREG/CR-2456, ORNL-5848, March 1982.

3. K. Carlson, R. Riemke, R. Wagner, J. Trapp, "Addition of Three-Dimensional Modeling," RELAP5/TRAC-B International Users Seminar, Baton Rouge, LA, November 4-8, 1991.
4. R. Riemke, "RELAP5 Multi-Dimensional Constitutive Models," RELAP5/TRAC-B International Users Seminar, Baton Rouge, LA, November 4-8, 1991.
5. K. Carlson, R. Riemke, R. Wagner, "Theory and Input Requirements for the Multi-Dimensional Component in RELAP5 for Savannah River Site Thermal-Hydraulic Analysis," EGG-EAST-9878, Idaho National Engineering Laboratory, July, 1992.
6. K. Carlson, C. Chou, C. Davis, R. Martin, R. Riemke, R. Wagner, "Developmental Assessment of the Multi-Dimensional Component in RELAP5 for Savannah River Site Thermal-Hydraulic Analysis," EGG-EAST-9803, Idaho National Engineering Laboratory, July, 1992.
7. K. Carlson, C. Chou, C. Davis, R. Martin, R. Riemke, R. Wagner, R. Dimenna, G. Taylor, V. Ransom, J. Trapp, "Assessment of the Multi-Dimensional Component in RELAP5/MOD2.5, Proceedings of the 5th International Topical Meeting on Nuclear Reactor Thermal-Hydraulics, Salt Lake City, Utah, USA, September 21-24, 1992.
8. P. Murray, R. Dimenna, C. Davis, "A Numerical Study of the Three Dimensional Hydrodynamic Component in RELAP5/MOD3," RELAP5 International Users Seminar, Boston, MA, USA, July, 1993.
9. G. Johnsen, "Status and Details of the 3-D Fluid Modeling of RELAP5," Code Application and Maintenance Program Meeting, Santa Fe, NM, October, 1993.
10. E. Tomlinson, T. Rens, R. Coffield, "Evaluation of the RELAP5/MOD3 Multidimensional Component Model, RELAP5 International Users Seminar, Baltimore, MD, August 29 – September 1, 1994.
11. A. Shieh, "1D to 3D Connection for the Nearly-Implicit Scheme," INEL Report, June, 1997.
12. K. Carlson, "1D to 3D Component Connection for the Semi-Implicit Scheme," INEL Report, June, 1997.
13. C. Davis, "Assessment of the RELAP5 Multi-Dimensional Component Model Using Data from LOFT Test L2-5," INEEL Report LDRD 3101, September, 1996.
14. R. M. Al-Chalabi, et al, "NESTLE: A Nodal Kinetics Code," Transactions of the American Nuclear Society, Volume 68, June, 1993.
15. H. Finnemann and A. Galati, "NEACRP 3-D LWR Core Transient Benchmark – Final Specifications," NEACRP-L-335 (Revision 1), January, 1992.
16. J. L. Judd, W. L. Weaver, T. Downar, J. G. Joo, "A Three Dimensional Nodal Neutron Kinetics Capability for RELAP5," Proceedings of the 1994 Topical Meeting on Advances in Reactor Physics, Knoxville, TN, April 11-15, 1994, Vol. II, pp 269-280.
17. H. Finnemann, et al, "Results of LWR Core Transient Benchmarks," Proceedings of the Joint International Conference on Mathematical Methods and Supercomputing in Nuclear Applications, Vol. 2, pg. 243, Kernforschungszentrum, Karlsruhe, Germany, April, 1993.